

Effects of disorder on electron-spin relaxation in β -alumina: A prototype glass

S. R. Kurtz and H. J. Stapleton

*Department of Physics and Materials Research Laboratory, University of Illinois at Urbana-Champaign,
Urbana, Illinois 61801*

(Received 7 January 1980)

Properties unique to disordered materials have been observed through electron paramagnetic resonance studies of a prototype glass. The electron-spin-relaxation rate of an irradiation-induced color center was measured in K, Li, and Na β -alumina, and revealed exceptionally fast relaxation with anomalous temperature and microwave frequency dependence. This behavior is quantitatively described by a mechanism involving the coupling of a color center to the phonon-induced relaxation of a nearby localized two-level tunneling state. A detailed comparison shows that our model is in agreement with earlier heat-capacity, thermal-conductivity, and dielectric-susceptibility measurements in β -alumina.

I. INTRODUCTION

Electron- and nuclear-spin-resonance data from amorphous materials have established that the relaxation rates are anomalously large and show unusual temperature dependences when compared to crystalline solids. Feldman *et al.*¹ observed this in their electron-spin-relaxation studies on atomic hydrogen in fused silica. Murphy² described their data by speculating the presence of "local vibrations" within the glass. Later similar anomalies were observed in the nuclear-spin-relaxation data of glasses.³⁻⁸ Measurements of the homogeneous fluorescence linewidth in rare-earth-doped glasses have also revealed an anomalous temperature dependence and a larger magnitude than observed in crystals containing the same ions.^{9,10} The results from these differing experiments display striking similarities, and the data obtained from any one type of these experiments is largely independent of the particular glass being studied. The facts suggest that these related phenomena are caused by interactions with localized-tunneling states (LTS), which have so successfully explained the low-temperature properties of amorphous materials.^{11,12} In previous papers^{13,14} we have proposed a quantitative model for the electron-spin relaxation in a glass utilizing the LTS theory. Lyo and Orbach¹⁵ have independently proposed a similar theory in which they seek to explain the fluorescence linewidth in glasses.

In order to test any model for spin relaxation in glasses, it is necessary to select a system in which one can estimate the magnitude of the LTS-spin interaction. It is also helpful to choose a material for which several low-temperature properties have been measured. Data from specific-heat, thermal-conductivity, and dielectric-susceptibility experiments provide an

approximate description of the tunneling-state system in a particular glass. For these reasons we have chosen β -alumina for our studies. In β -alumina, the disorder is confined to the two-dimensional conduction planes.¹⁶ This simplifies identification of the tunneling species and estimation of its coupling to the spins. Measurements by Anthony and Anderson of the thermal conductivity,¹⁷ specific heat,¹⁸ and low-frequency dielectric susceptibility,¹⁹ of Li, Na, K, and Ag β -alumina at low temperature have established that these materials are glasses at low temperature. The low-temperature dielectric properties of Na β -alumina at 11.5 GHz also exhibit saturation effects characteristic of the presence of two-level, localized-tunneling states.²⁰

Estimates of the LTS system parameters, which can explain the low-temperature data of the β -aluminas, have been published.¹⁹ With such data we have sufficient information to quantitatively test the predictions of our relaxation model. Such a rigorous test of a model for electron-spin relaxation in a glass has not been possible previously.

In this paper, we present our results of electron-spin-relaxation measurements on a color center located in the conduction plane of Li, K, and Na β -alumina, and we interpret our data with a detailed model for spin relaxation via the LTS. The experiment requires the production of color centers in the conduction plane of the β -alumina by low-temperature irradiation, identification of the centers by electron paramagnetic resonance (EPR), and measurements of the electron-spin-relaxation rate of the color center using the pulse saturation and recovery technique. Details of the experimental procedures are discussed in Sec. II. The theory we use for our analysis of the data combines our earlier model^{13,14} with the work of Lyo and Orbach,¹⁵ and is presented

in Sec. III. A detailed comparison of the relaxation model with our data, the low-temperature data on β -alumina, and other relaxation data in glasses, is presented in Sec. IV. In Sec. V we state our conclusions.

II. EXPERIMENTAL PROCEDURES AND RESULTS

β -alumina samples, originally grown by Union Carbide Corporation,²¹ were provided by Bates of the Oak Ridge National Laboratory and Anderson of this laboratory. The potassium and lithium salts had been synthesized by Anthony²² using repeated ion exchange, employed in his measurements,¹⁷⁻¹⁹ and loaned to us. The color centers were produced by irradiation at liquid-nitrogen temperatures using a Van de Graaf accelerator. All the samples were stored in an anhydrous environment and as a further precaution, the sample of Li β -alumina was dehydrated before irradiation by heating to 300°C for 48 h in a vacuum. A titanium foil was in front of the samples during the electron irradiation which was typically a dose of 10^{13} – 10^{14} electrons at 1.5 MeV energy. After irradiation the samples exhibited a dark-blue coloration until they were allowed to warm to room temperature for a short time in a dry box. This room-temperature annealing destroyed the blue coloration and left the nearly colorless sample with an electron-paramagnetic-resonance spectrum similar to that shown in Fig. 1. Except for additional brief periods

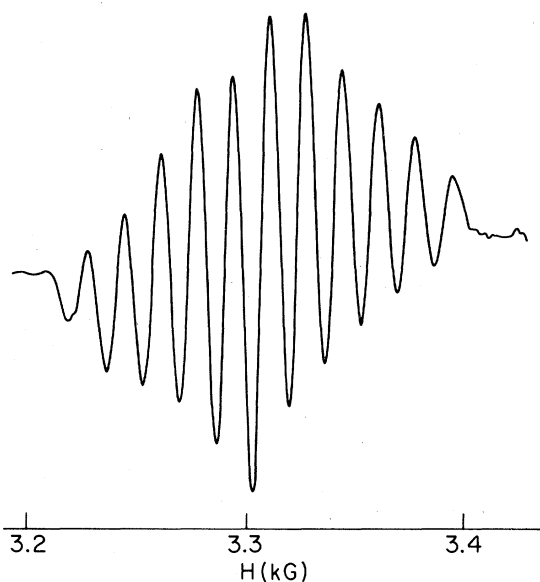


FIG. 1. Derivative of the EPR spectrum from a color center in the conduction plane of Na β -alumina as measured at 77 K and 9.3 GHz, with \vec{H} parallel to the c axis. A similar EPR spectrum appears in K β -alumina.

of warming while loading or unloading the samples into the microwave cavities, all samples were stored in liquid nitrogen.

The absorption-derivative spectrum shown in Fig. 1 exhibits an 11-line spectrum with intensity ratios of 1:2:3:4:5:6:5:4:3:2:1. This is the characteristic signature of an electron spin of $\frac{1}{2}$ interacting with two equivalent $I = \frac{5}{2}$ nuclei. O'Donnell, Barklie, and Henderson²³ have independently observed this spectrum and report the center to be axially symmetric about the hexagonal crystalline axis with principle g factors of $g_{\parallel} = 2.0076$ and $g_{\perp} = 2.0032$. The center therefore lies in the mirror (i.e., conduction) plane, midway between two aluminum ($I = \frac{5}{2}$) nuclei. The fact that the g factors are so close to the free-electron value suggests that the wave function of the paramagnetic species is p like or s like. An O^{-} ion would be p like, but O'Donnell *et al.* argue convincingly that this cannot be the situation in this case. Under axial symmetry the g value of a p orbital should equal that of a free electron when the magnetic field is parallel to the p lobe, and differ from the free-electron value when the field is perpendicular to the lobe. This center shows significant deviation in the g factor from 2.0023 when the external field is parallel to the crystalline symmetry axis. That would place the p lobe in the conduction plane and produce a very small contact hyperfine interaction with the aluminum nuclei above and below the conduction plane. This is contrary to the large isotropic aluminum hyperfine interaction observed experimentally. O'Donnell *et al.* therefore reject the model of an O^{-} ion, and suggest instead that the center is an electron trapped at an O^{2-} vacancy. Such O^{2-} vacancies would aggravate the problem of charge neutrality in these alkali-rich salts, but the concentration of these color centers is reported to saturate with increased irradiation at a level of 10^{-4} per unit cell.²³ The evidence is strongly in favor of an F^{+} center at the O(5) site¹⁶ in the β -alumina. The β -alumina structure is shown in Fig. 2. The O(5) site is in the conduction plane, 0.168 nm from the aluminum nuclei and 0.323 nm from the sodium nuclei in the perfect crystal. From the EPR data, we cannot distinguish this F^{+} center from an Al- F^{+} -Al bridge at a midoxygen site replacing a charge-compensating oxygen. While the EPR spectrum of irradiated K β -alumina was similar to that of the Na β -alumina in Fig. 1, the EPR spectrum of irradiated Li β -alumina as shown in Fig. 3, suggests that in this salt the aluminum- F^{+} hyperfine interaction varies within the crystal. This may be due to displacement of the Li ion out of the conduction plane which in turn distorts the symmetry of the aluminum nuclei about the F^{+} center. Evidence for lithium motion out of the plane has been reported from dielectric susceptibility and Raman data.^{19,24} Alternatively, absorption of water into the conduction plane of Li β -alumina may break the symmetry. Ag

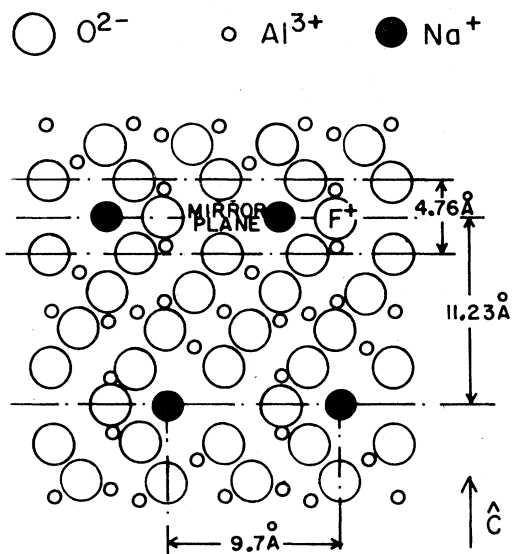


FIG. 2. Structure of stoichiometric Na β -alumina with the probable position of the F^+ color center indicated within the conduction (mirror) plane. Above and below the F^+ center are the two equivalent aluminum nuclei which produce the observed hyperfine lines in the EPR spectra. A Na^+ cation is located 0.32 nm from the F^+ center.

β -alumina did not exhibit the F^+ center after irradiation, and therefore is not included in this relaxation study. Additional details concerning the EPR and electron-nuclear double resonance (ENDOR) spectra of these salts will be published separately.

The spin-lattice relaxation rates were measured at 9.5 and 16.5 GHz using the pulse saturation and recovery technique. Both spectrometers utilized broad-band (dc to 10 MHz) superheterodyne detection and signal averaging. Most of the details concerning the present arrangement of the variable tem-

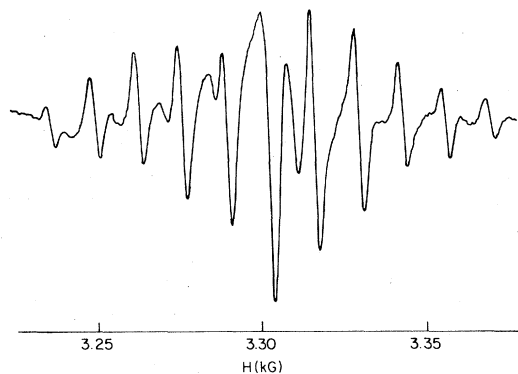


FIG. 3. Derivative of the EPR spectrum from a color center in the conduction plane of Li β -alumina as measured at 77 K and 9.3 GHz, with \vec{H} parallel to the c axis. Features of the eleven-line pattern displayed in Fig. 1 are still visible.

perature, X- and Ku-band pulsed spectrometers have been published,²⁵ with the exception that currently in both spectrometers there are two 50-dB microwave switches, operating 180° out of phase, in order to protect the receivers during the saturating pulse. Sample temperatures were measured and controlled to within a few millikelvin using a germanium resistance thermometer in one arm of a low-frequency bridge circuit whose signal unbalance was phase sensitively detected and used to drive a 500-ohm heater wound around the microwave cavity. The cavity was isolated from the helium bath by a surrounding copper can and thinwall stainless-steel waveguide. Helium gas was admitted into the can as a low-pressure exchange gas. Controlled temperatures to about 25 K were possible with this arrangement.

After signal averaging, the recovery could be displayed on a scope directly or after logarithmic amplification. This yielded immediate, but crude measurements of the relaxation rates as a function of temperature during the data-taking process. The data were recorded on paper tape or a magnetic floppy disk for more detailed analysis later. It should be noted that the recoveries were seldom truly exponential in time. The reason is that the observed relaxation rate of the F^+ center represents an average value, as will become evident later. Our data should be construed as representative of the recovery rate between times at which the signal is 60 and 90% recovered to its thermal-equilibrium value, and care was taken to ensure that these reported values were independent of the duration and amplitude of the saturating pulses. All published recovery times were measured at the same point in the hyperfine spectrum, with the magnetic field parallel to the c axis, but away from the central peak in order to avoid overlapping any additional resonance lines associated with g values of 2.00. However, the observed relaxation rates appeared to be independent of the point in the hyperfine spectrum where the experiment was performed, including the complicated Li β -alumina EPR spectrum.

A typical temperature dependence of these relaxation data is shown in Fig. 4. Several unusual features are apparent. At low temperatures the relaxation rate appears to be essentially temperature independent. At higher temperatures the rate varies faster than T initially, but becomes nearly linear at the highest temperatures for which we have data. An examination of these sodium data taken at the two microwave frequencies reveals another anomaly: the relaxation rate is almost independent of the microwave frequency. There appears to be a slight reduction of the rate with increased microwave frequency. These properties are not characteristic of the accepted relaxation mechanism of an F center in a crystalline material due to phonon modulation of ligand hyperfine interactions.²⁶ This leads to a one-phonon, direct re-

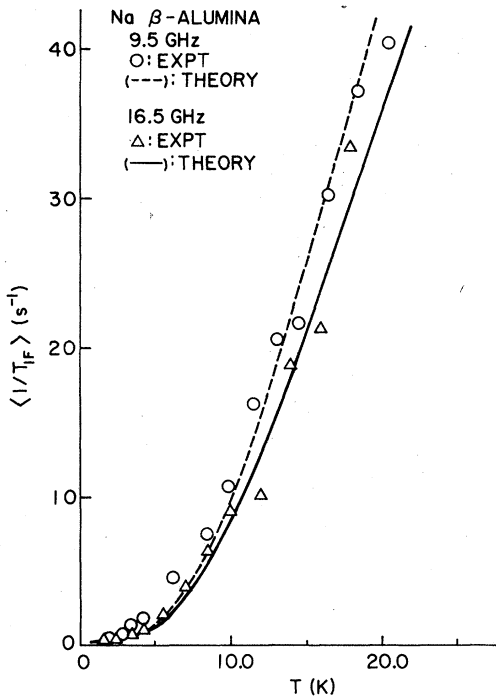


FIG. 4. Spin-relaxation rate of the color center in Na β -alumina as measured at microwave frequencies of 9.5 and 16.5 GHz. The curves (dashed and solid lines) are the result of the model described in the text.

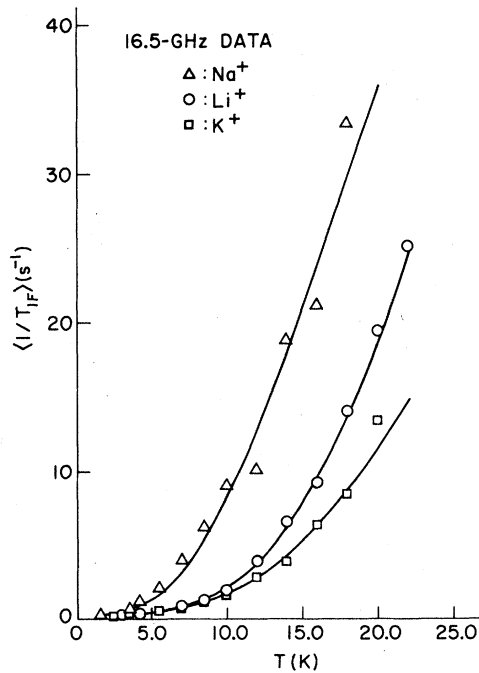


FIG. 5. Spin-relaxation rate of the color center of Na, Li, and K β -alumina as measured at a single microwave frequency of 16.5 GHz. The curve through the data for each sample results from the model described in the text.

laxation rate varying as $\nu^2 T$ at the lowest temperatures. At higher temperatures it results in a two-phonon Raman rate varying as $\nu^0 T^7 J_6(\Theta_D/T)$, where J_6 is a transport integral,²⁷ and Θ_D is the Debye temperature of the solid. For small values of Θ_D/T this Raman rate will vary at $\nu^0 T^2$ as expected for a two-phonon process in the classical limit. For large values of Θ_D/T , the transport integral becomes a constant resulting in a $\nu^0 T^7$ Raman relaxation rate.

The relaxation data from β -alumina cannot be explained by conventional phonon processes. If one attempts to explain the data of Fig. 4 by attributing the rates above 10 K to a direct process, varying as T and the low-temperature data to a temperature-independent cross-relaxation mechanism, then the linear portion of the curve would have to extrapolate through the origin, which it clearly does not. In addition, the magnitude of the relaxation rate at any temperature is about three orders of magnitude faster than usually observed for F centers in crystalline materials. These same characteristics are observed in the F^+ -center relaxation data for Na, Li, and K β -alumina shown in Fig. 5. In order to explain our relaxation data, we must include additional relaxation mechanisms associated with the presence of the LTS system. In Sec. III we discuss this.

III. MODEL FOR ELECTRON-SPIN RELAXATION BY LOCALIZED-TUNNELING STATES

The localized-tunneling-state model assumes atoms or groups of atoms in amorphous materials reside in asymmetric double-well potentials, and tunneling occurs through the barrier separating the two wells. This results in two closely spaced energy levels. The unperturbed LTS Hamiltonian in the nondiagonal basis of two separate wells will be denoted with a superscript prime and is given by

$$\mathcal{H}'_0 = \frac{1}{2} \begin{pmatrix} \xi & \Delta \\ \Delta & -\xi \end{pmatrix}, \quad (1)$$

where ξ is the asymmetry of the potential wells, and Δ is an overlap energy given by $\hbar \omega_0 e^{-\lambda}$. Here $\hbar \omega_0$ is the ground-state energy of an isolated potential well and λ equals $(2mV)^{1/2} d/\hbar$, where V is the barrier height, d the well separation, and m is the mass of the tunneling unit. In the diagonal (unprimed) basis, the Hamiltonian becomes

$$\mathcal{H}_0 = \frac{1}{2} \begin{pmatrix} E & 0 \\ 0 & -E \end{pmatrix}, \quad (2)$$

where E is the energy splitting between the two levels and equals $(\xi^2 + \Delta^2)^{1/2}$. A fundamental property of the LTS theory is that there exists an almost constant and broad distribution of E values up to a cutoff E_{\max}/k of the order of 10–100 K. It is generally assumed that the LTS distribution can be described by

a density of states given by²⁸

$$P(E, \Delta) = \frac{P(E)}{\Delta[1 - (\Delta/E)^2]^{1/2}}, \quad (3)$$

where $P(E)$ is very weakly dependent upon E .

The form and magnitude of the tunneling state-phonon interaction dominates the physics of acoustic, dielectric, and relaxation phenomena in insulating glasses. Recently it has been proposed that this strong interaction may explain the broad distribution of tunneling-state energies common to all glasses.²⁹ In the diagonal basis this tunneling state-phonon interaction becomes

$$\mathcal{H}_{T-PH} = \frac{1}{2E} \begin{pmatrix} \xi \frac{\partial \xi}{\partial e} + \frac{\Delta \partial \Delta}{\partial e} & \xi \frac{\partial \Delta}{\partial e} - \frac{\Delta \partial \xi}{\partial e} \\ \xi \frac{\partial \Delta}{\partial e} - \frac{\Delta \partial \xi}{\partial e} & \xi \frac{\partial \xi}{\partial e} - \frac{\Delta \partial \Delta}{\partial e} \end{pmatrix} e, \quad (4)$$

where e is a strain. Further approximations to Eq. (4) are discussed later.

Formulation of the electron spin-LTS interaction requires speculation on the location and identification of the tunneling unit. In β -alumina, the observed low-temperature properties are strongly dependent upon the cation present in the conduction plane. We therefore assume that some of the cations in the conduction plane are tunneling. It is improbable that these are the only tunneling units in the material. The coupling of the F^+ center to the LTS is assumed to be a Fermi contact hyperfine (hf) interaction with a cation nucleus tunneling a distance d through the

barrier. For an F^+ center, $|\psi|^2$ at the cation nucleus scales roughly as $Z^{3/2}/R_0^3$ where Z is the atomic number of the ligand.³⁰ This allows us to write the spin-LTS interaction for an F^+ in contact with a tunneling cation characterized by an energy splitting E , as

$$\mathcal{H}'_{S-T} = A \bar{I} \cdot \bar{S} \frac{3d}{2R_0} \begin{pmatrix} -1 & 0 \\ 0 & +1 \end{pmatrix}, \quad (5)$$

or in the diagonal basis as

$$\mathcal{H}_{S-T} = A \bar{I} \cdot \bar{S} \frac{3d}{2R_0 E} \begin{pmatrix} -\xi & \Delta \\ \Delta & \xi \end{pmatrix}. \quad (6)$$

The strength of the contact hf interaction between the F^+ center and the nearest-neighbor sodium nucleus was determined to be $A/h \approx 8$ MHz from our unpublished ENDOR data. Assuming that the cation is at a Beevers-Ross site, 0.32 nm from the O(5) site, the EPR spectrum and the scaling law predict a coupling of 5 MHz. Average values of d can be estimated from dielectric-susceptibility data.^{19,20}

If we denote

$$\begin{aligned} |i\rangle &= |+, \psi_+, \dots, \eta_\alpha, \dots\rangle, \\ |f\rangle &= |-, \psi_-, \dots, \eta_\alpha + 1, \dots\rangle \end{aligned} \quad (7)$$

as initial and final states, in which $|\pm\rangle$, $|\psi_\pm\rangle$, and $|\eta_\alpha\rangle$ are electron spin, LTS, and phonon states, respectively, then the interaction Hamiltonians of Eqs. (4) and (6) yield the following transition rate

$$\begin{aligned} W_{if} = \frac{2\pi}{\hbar} \sum_{\alpha} & \left| \frac{\langle -, \psi_- | \mathcal{H}_{T-S} | +, \psi_+ \rangle \langle \psi_+, \eta_\alpha + 1 | \mathcal{H}_{T-PH} | \psi_+, \eta_\alpha \rangle}{-\hbar \omega_\alpha} + \frac{\langle -, \psi_- | \mathcal{H}_{T-S} | +, \psi_- \rangle \langle \psi_-, \eta_\alpha + 1 | \mathcal{H}_{T-PH} | \psi_+, \eta_\alpha \rangle}{-\hbar \omega_\alpha + E} \right. \\ & \left. + \frac{\langle \psi_-, \eta_\alpha + 1 | \mathcal{H}_{T-PH} | \psi_+, \eta_\alpha \rangle \langle -, \psi_+ | \mathcal{H}_{T-S} | +, \psi_+ \rangle}{\delta} + \frac{\langle \psi_-, \eta_\alpha + 1 | \mathcal{H}_{T-PH} | \eta_\alpha, \psi_- \rangle \langle -, \psi_- | \mathcal{H}_{T-S} | +, \psi_+ \rangle}{E + \delta} \right|^2 \\ & \times (1 + e^{E/kT})^{-1} \delta_D(\hbar \omega_\alpha - E - \delta). \end{aligned} \quad (8)$$

Here δ is the electronic Zeeman-energy splitting, δ_D is the Dirac δ function, and the quantum numbers of all nuclear-spin states have been suppressed. By considering the additional pair of initial and final states given by

$$|i'\rangle = |+, \psi_-, \dots, \eta_\alpha + 1, \dots\rangle, \quad |f'\rangle = |-, \psi_+, \dots, \eta_\alpha, \dots\rangle, \quad (9)$$

one obtains the following relaxation rate of an F^+ center, where Γ , the energy width of an intermediate LTS or phonon state, has been included and E is assumed to be much larger than δ :

$$\frac{1}{T_{1F}} = W_{if} + W_{fi} + W_{i'f'} + W_{f'i'} = \frac{D \operatorname{sech}^2(E/2kT)}{4\tau' E^4} \left[\frac{\Delta^2 (\xi \frac{\partial \xi}{\partial e} + \Delta \frac{\partial \Delta}{\partial e})^2}{E^2 + \Gamma^2} + \frac{\xi^2 (\xi \frac{\partial \Delta}{\partial e} - \Delta \frac{\partial \xi}{\partial e})^2}{\delta^2 + \Gamma^2} \right], \quad (10)$$

where

$$D = \frac{5}{2} \left(\frac{3Ad}{2R_0} \right)^2 \quad (11)$$

and

$$\begin{aligned} \frac{1}{\tau} &= \frac{(\xi \partial \Delta / \partial e - \Delta \partial \xi / \partial e)^2}{4E^2 \tau'} \\ &= \frac{1}{2\pi \hbar^4 \rho} \left(\frac{2}{v_T^5} + \frac{1}{v_L^5} \right) \\ &\quad \times \frac{1}{4} E \left[\xi \frac{\partial \Delta}{\partial e} - \Delta \frac{\partial \xi}{\partial e} \right]^2 \coth \left(\frac{E}{2kT} \right). \end{aligned} \quad (12)$$

Equation (12) represents the relaxation rate, $1/\tau$, of a LTS which results from a direct, one-phonon process. In Eq. (12), v_T and v_L represent the transverse- and longitudinal-acoustic-phonon speeds, respectively, and ρ is the crystalline mass density. This expression assumes a range of $1/\tau$ values for a single value of E , but the results of our relaxation model are insensitive to this distribution since we

$$\left\langle \frac{1}{T_{1F}} \right\rangle = \int_0^{E_{\max}} \int_{\Delta_{\min}}^E \frac{1}{T_{1F}} P(E, \Delta) d\Delta dE / \int_0^{E_{\max}} \int_{\Delta_{\min}}^E P(E, \Delta) d\Delta dE. \quad (13)$$

In order to facilitate a comparison of our results with the data of Anthony and Anderson,¹⁹ we fitted our data to a LTS density of states such that

$$\int_{\Delta_{\min}}^E P(E, \Delta) d\Delta = P_M \left(\frac{E}{kT_N} \right)^{0.2} + P_N \left(\frac{E}{kT_N} \right)^3, \quad (14)$$

with Δ_{\min}/E equal to 10^{-3} , T_N equal to 1 K, and a cutoff at E_{\max} . P_M and P_N are constants determined from fitting the data, but P_M is much greater than P_N .

The spin-relaxation mechanism we have described is a process requiring one LTS and one phonon. It is shown schematically in Fig. 6. The rapid LTS relaxation rate $1/\tau$ is represented by the solid line and involves only a tunneling-state transition. This mechanism is assumed strong enough to keep the LTS system in thermal equilibrium with the phonon bath at all times. Electron-spin relaxation proceeds via the pathways indicated by the dotted lines of Fig. 6. These transitions are weakly allowed by the hyperfine interaction which admixes the basis states, resulting in simultaneous spin and LTS transitions through the emission or absorption of a phonon. Our physical picture of relaxation with the coupled spin and LTS systems is analogous to nuclear relaxation in the presence of paramagnetic impurities in the fast-diffusion limit.³¹ Figure 6 also illustrates this nuclear-relaxation phenomenon for nuclei, with a Zeeman splitting δ , which are weakly coupled to rapidly relaxing electrons, with a Zeeman splitting $E \gg \delta$. As before, nuclear relaxation occurs by the transitions indicated by the dotted lines, and these transitions are allowed by spin-function admixtures induced by the weak dipole-dipole interaction between the two spin systems.

eventually average over the values of Δ and ξ . The factor of $\frac{5}{2}$ in Eq. (11) results from averaging over the $I = \frac{3}{2}$ nuclear-spin matrix elements.

More precisely, $1/T_{1F}$ in Eq. (10) represents the electron-spin-relaxation rate of an F^+ center adjacent to a tunneling cation with LTS parameters Δ , ξ , $\partial \Delta / \partial e$, and $\partial \xi / \partial e$. Since there is a distribution of LTS parameters, it is necessary to average $1/T_{1F}$ over this distribution in order to obtain a measurable relaxation rate. Based on estimates of the LTS density, it is probable that only about 10% of the F^+ centers are strongly coupled to any LTS.¹⁹ In this situation, the bulk of the F^+ centers must relax via spin diffusion to the faster relaxing centers which are in hf contact with a LTS. Assuming rapid spin diffusion, because of a negligible diffusion barrier, the observed average electron-spin-relaxation rate is

Two of the interesting properties of this model are the different magnetic-field and temperature dependences predicted by the two terms in Eq. (10). If we assume that the density of tunneling states, $P(E)$, is a constant up to some cutoff E_{\max} , and that Γ is much smaller than E , the LTS energy splitting, then the first term in Eq. (10) predicts that $\langle 1/T_{1F} \rangle \propto H^0 T^2$ for $kT \ll E_{\max}$. With the additional as-

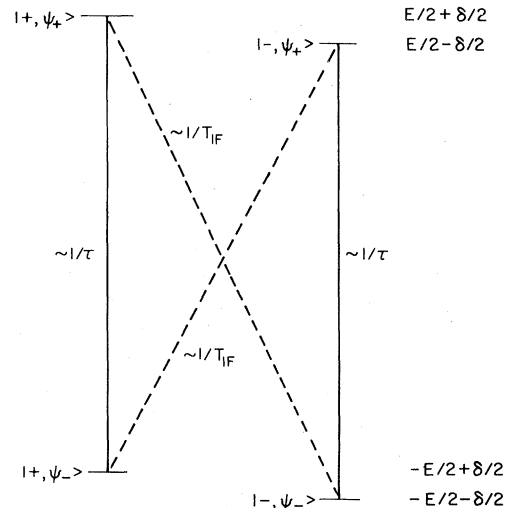


FIG. 6. Schematic diagram of the energy levels and product wave functions for a coupled electron spin (\pm)-localized tunneling-state (ψ_{\pm}) system. The solid lines indicate transitions which contribute to the relaxation rate $1/\tau$ of the localized tunneling state, and the dashed lines indicate transitions which contribute to the slower electron-spin-relaxation rate $1/T_{1F}$.

sumption that $\delta = g\mu_B H \gg \Gamma$, the second term predicts in contrast that $\langle 1/T_{1F} \rangle \propto H^{-2}T^4$. Both terms predict a linear temperature dependence at higher temperatures, where $kT \gtrsim E_{\max}$. Therefore, at low temperatures our model predicts $\langle 1/T_{1F} \rangle \propto T^{2-4}$. This result is confirmed by our data as shown in Fig. 7. In this diagram, each set of data was fitted to a function of the form

$$\langle 1/T_{1F} \rangle = BT^n + C, \quad (15)$$

where C is a positive constant. The $T^{3.48}$ and $T^{3.62}$ behavior of the Li and K β -alumina data suggests that unless $P(E) \propto E^{1.5}$ for $1 \leq E/k \leq 10$ K, the second term in Eq. (10) must contribute significantly to the F^+ relaxation rate in these materials. None of the data for other experiments supports the existence of a strongly E -dependent LTS density of states in this region.^{19,20} The $T^{2.02}$ and $T^{2.77}$ power-law fits of the Na data at X - and Ku -band frequencies may reflect a lower cutoff value of E_{\max}/k , the values of which have been reported as 65, 80, and 130 K for Na, K, and Li β -alumina, respectively.¹⁹ A lower cutoff energy tends to linearize the T dependence at a lower temperature. Another factor which supports the dominance of the second term in Eq. (10) is the small, but clearly perceptible, frequency dependence of

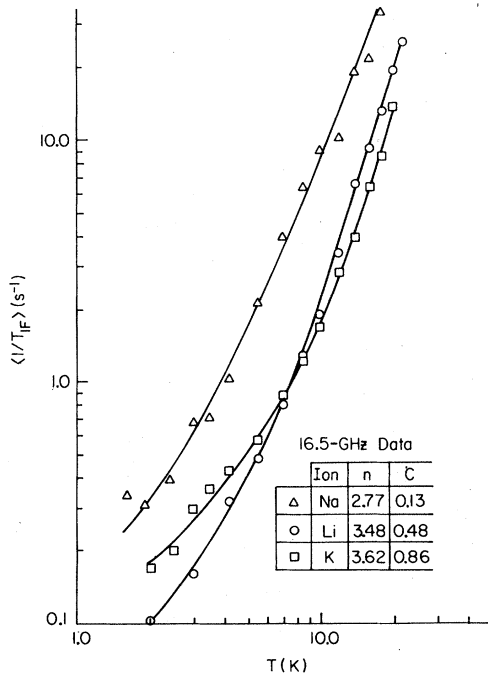


FIG. 7. $\log \langle 1/T_{1F} \rangle$ vs $\log T$ for Na, Li, and K β -alumina as measured at a microwave frequency of 16.5 GHz. The curves and table result from fitting the data to the function described by Eq. (15) of the text. A similar fit of the Na β -alumina data at 9.5 GHz is not shown, but it produced a $T^{2.02}$ temperature dependence for $\langle 1/T_{1F} \rangle$.

$\langle 1/T_{1F} \rangle$ shown in Fig. 4. The Ku -band relaxation data is consistently slower than the corresponding X -band data. However, the field dependence is much reduced from H^{-2} , a result predicted only in the limit that $\delta \gg \Gamma$.

Lyo and Orbach¹⁵ have proposed that the first and fourth terms in Eq. (8) can explain the optical homogeneous linewidth^{9,10} which varies as T^2 in rare-earth-doped glasses. Considering only scattering processes in which the ion remains in the same electronic state, we must change $|-\rangle$ to $|+\rangle$ in the final state and consider it one of the electronic levels involved in the optical transition. An examination of the intermediate states in Eq. (8) shows that only the first and fourth terms, due to Lyo and Orbach, are then permitted.

In Eq. (8), the intermediate states are such that only one of the two Hamiltonian operators, \mathcal{H}_{T-S} or \mathcal{H}_{T-PH} , is off-diagonal with respect to the LTS. Another spin-relaxation mechanism is possible in which both of these operators are off-diagonal with respect to the tunneling states. The resulting temperature dependence of this mechanism is identical to that of an ordinary one-phonon direct process, i.e., proportional to T for $kT \gg \delta$.

The only remaining T_1 process involving these interactions in first order is the resonant cross relaxation between a spin and LTS for which $E = \delta$. Assuming: (i) that the resonant tunneling states remain in thermal equilibrium with the lattice as the spins and resonant tunneling states undergo mutual "flip-flop" transitions, and (ii) that a rapid spin-diffusion rate can be ascribed to the spin system, then the resulting relaxation rate is independent of temperature. Such resonant pairs of spins and tunneling states will be very rare, but also very effective in bringing the spin system to thermal equilibrium at low temperatures where other processes freeze out.

Another relaxation mechanism is a two LTS process proposed by Reinecke and Ngai⁷ to explain nuclear relaxation in glasses. We do not consider this process a reasonable explanation for the observed electron-spin-relaxation data for two reasons. First, it requires the improbable situation of two LTS states having an energy difference δ , to be coupled strongly to the same F^+ center. Second, the predicted relaxation rate for this mechanism varies as T if $P(E)$ is a constant and $kT \ll E_{\max}$.

We have considered two possible temperature dependences in order to account for the observed relaxation rates at the lowest temperatures, where the mechanism involved in Eq. (13) becomes very weak. We have assumed either a constant rate, C , or one linear in temperature, GT . The fit of the data at the higher temperatures is only slightly affected by this choice, and we report here only those fits which include the GT term.

In addition to the LTS system, excess vibrational

states have been observed in β -alumina. Infrared-spectra,³² Raman-scattering data,³³ and heat-capacity results³⁴ were explained by speculating the existence of Einstein oscillator states due to cation motion within the conduction plane. These excitations have well-defined energies instead of the broad distribution characteristic of the LTS. If the spins interacted with a Debye-phonon system augmented by these Einstein oscillators instead of the LTS, the expression for the relaxation rate would be $\langle 1/T_{1F} \rangle \propto e^{-E'/kT}$ for $E' \gg kT$, where E' is the Einstein oscillator energy. Our data are not described by this temperature dependence. Also infrared, Raman, and heat-capacity experiments all failed to observe Einstein oscillator states of comparable energy in Li β -alumina, but we observe the same spin-relaxation phenomena in Li β -alumina as in Na and K β -alumina. For these reasons, we insist that the LTS and not the excess vibrational states allow the phonons to relax the F^+ centers. It is possible that these excess vibrational states also interact with the LTS producing a slightly different spin-relaxation temperature dependence than predicted by a simple Debye-phonon spectrum, but we have not attempted to account for this effect in our data analysis.

IV. COMPARISON BETWEEN THEORY AND EXPERIMENT

In this section we make basic assumptions about the nature of Γ and \mathcal{K}_{T-PH} , and based on these assumptions we estimate values of the LTS parameters which provide a quantitative description of our electron-spin-relaxation data. Using the theory presented in the previous section, we can then check our LTS parametrization with the results from low-temperature bulk measurements on the β -alumina. Through this process, we finally obtain a self-consistent explanation of the electron-spin-relaxation phenomena in glasses, and we reconfirm properties of the LTS model previously observed through bulk measurements only.

It is convenient to begin this discussion by assuming that Γ is due to a large LTS linewidth, i.e.,

$$\Gamma_{LTS} \propto \hbar \left(\frac{1}{\tau} + \frac{1}{T_2} \right). \quad (16)$$

Here $1/T_2$ is an LTS-LTS relaxation rate, and it has been widely studied through a variety of acoustic and dielectric experiments.^{35,36} Although the origin of $1/T_2$ is not completely understood, it is believed to be only weakly dependent on T and E ,^{4,37} and at $T = 1.5$ K and $E/h = 9$ GHz, it has been estimated at 2×10^9 s⁻¹ in borosilicate BK7.³⁸ The LTS-lattice relaxation rate is measured indirectly in any resonant contribution to dielectric susceptibility or thermal

conductivity, and in practically all glasses it is found to be less than about 10^6 s⁻¹ for an E/h of 9 GHz and at a temperature of 2 K. In sodium β -alumina, dielectric saturation has been observed,²⁰ and this allowed the investigators to estimate τT_2 at 6×10^{-11} s² for an E/h of 11.5 GHz and a temperature of 1 K. All this experimental evidence indicated that δ is much larger than Γ_{LTS} in the temperature region of our experiments, where $\delta/h \approx 10$ GHz.

Based on the temperature dependence and weak-field dependence exhibited in our electron-spin-relaxation data, it would still be possible to reproduce our results with $\delta \gg \Gamma$ if the two terms of Eq. (10) were of comparable size. The H and T dependence of each set of data could then be fit by adjusting the relative contributions of each of these terms. Under these approximations

$$\frac{1}{T_{1F}} \propto \frac{\Delta^2(\xi \partial \xi / \partial e + \Delta \partial \Delta / \partial e)^2}{E^2} + \frac{\xi^2(\xi \partial \Delta / \partial e - \Delta \partial \xi / \partial e)^2}{\delta^2}. \quad (17)$$

Making the usual assumption that $\partial \xi / \partial e \gg \partial \Delta / \partial e$ would lead to the result that the second term of Eq. (17) is much larger than the first if $E \gg \delta$. In order to make the contribution from the first term significant, one must make the diagonal components of \mathcal{K}_{T-PH} larger while diminishing the off-diagonal elements. This can be accomplished by setting $\partial \xi / \partial e \approx \partial \Delta / \partial e$. However, this same LTS-phonon interaction describes acoustic attenuation and thermal conductivity in glasses. In these experiments "resonant"-scattering processes are produced by the contribution of the off-diagonal components of \mathcal{K}_{T-PH} , and "relaxation"-scattering processes are caused by the diagonal components.²⁸ The assumption that $\partial \xi / \partial e \gg \partial \Delta / \partial e$ produces the correct relative sizes of the "relaxation" and "resonant" processes observed in acoustic measurements to within a factor of 10.³⁶ In order to force the two terms in Eq. (17) to contribute equally at 10 K, with $E_{max}/k \approx 50$ K, and $\delta/h \approx 10$ GHz, the diagonal and off-diagonal elements of \mathcal{K}_{T-PH} must be adjusted so as to enhance the relaxation-scattering processes over the resonant-scattering processes by a factor of 1000 or more. Such a large asymmetry in the relative strengths of the two processes has not been observed experimentally in any glass, including β -alumina. Therefore, under the assumption that $\delta \gg \Gamma$, the second term in Eq. (17) dominates, and our model would then predict a much stronger magnetic-field dependence than is observed.

Another contribution to Γ could arise from short phonon lifetimes. Here $\Gamma_{PH} \approx \hbar \nu / l$, where ν is an acoustic-phonon velocity and l is a phonon mean free path. In a perfect crystal l is limited by the finite crystal size and weak phonon-phonon scattering

resulting from anharmonic terms in the lattice potential. In a glass, however, l is limited by the structural disorder of the material, at least for phonons with wavelengths comparable to the size of a unit cell of the glass. Using this physical picture, Kittel³⁹ explained the thermal-conductivity data of glasses by suggesting a constant, temperature-independent mean free path $l_0 \approx 10^{-7}$ cm for phonons with $\omega/2\pi \gtrsim 100$ GHz. These higher-frequency phonons are just those responsible for the relaxation of the higher-energy tunneling states, which in turn are responsible for the spin relaxation of the F^+ center in our model. With $v \approx 10^5$ cm/s, $\Gamma_{PH}/h \approx v/2\pi l_0$ is of the order of 100 GHz, and under these conditions $\Gamma_{PH} \gtrsim \delta$ since $\delta/h \approx 10$ GHz in our experiments. Therefore, the short phonon lifetimes observed in glasses can explain the weak magnetic-field dependence displayed by our data. Defining $(\frac{1}{2})\partial\xi/\partial e = \gamma$, and assuming $\partial\Delta/\partial e \approx 0$ (Ref. 28) we rewrite Eq. (10) as

$$\frac{1}{T_{1F}} = \frac{D \operatorname{sech}^2(E/2kT)\xi^2}{\tau E^2} \left(\frac{1}{E^2 + \Gamma_{PH}^2} + \frac{1}{\delta^2 + \Gamma_{PH}^2} \right) \quad (18)$$

It must be noted that we have explained the magnetic-field dependence with a value of Γ_{PH} such that

$\Gamma_{PH}/\hbar \gg 1/\tau$. In so doing we have assumed that the scattering processes which determine Γ_{PH} for the high-energy phonons do not involve the LTS system, and these scattering processes do not efficiently produce electron-spin transitions.

When Eq. (18) is applied to electron-spin relaxation in glasses, the relative sizes of E , Γ_{PH} , and δ are such as to make the second term dominant. The solid lines in Figs. 4 and 5 are the result of using Eq. (18) to calculate $\langle 1/T_{1F} \rangle$. The parameters used in these calculations are displayed in Table I along with estimates of the same parameters determined by Anthony and Anderson in the analysis of their data on β -alumina.¹⁹ In these fits of our data, the first term in Eq. (18) contributes less than 1% to the predicted relaxation rates.

There are too many adjustable parameters in the LTS model of glasses to allow a unique determination of these quantities from an analysis of relaxation data alone. The same can be said regarding most measurements on glasses. What can be accomplished is to produce a fit of the data in which the resulting parameters from all available experiments can be compared. For this reason we have adopted the parametrization scheme of Anthony and Anderson,¹⁹ but we emphasize that it is not a unique description of the LTS system in β -alumina. However, the

TABLE I. Summary of the parameters for Na, Li, and K β -alumina used to generate the curves in Figs. 4 and 5. All parameters are defined in the text. Results of Anthony and Anderson (Footnote a) are included for comparison.

Parameter	Units	Na	Li	K	Footnote
ρ	g cm ⁻³	3.22	3.14	3.33	a
v_T	10 ⁵ cm s ⁻¹	3.8	4	4.3	a
v_L	10 ⁵ cm s ⁻¹	9.1	9	9.5	a
Δ_{\min}/E	...	10 ⁻³	10 ⁻³	10 ⁻³	a
P_M	10 ³³ erg ⁻¹ cm ⁻³	2.4	4.9	1.2	a
P_N	10 ²⁹ erg ⁻¹ cm ⁻³	2.5	0.0	0.15	b
E_{\max}/k	K	40	90	80	b
γd	10 ⁻⁸ cm eV	0.12	0.40	0.18	b
$A(R_0, \mu, Z)$	10 ⁶ Hz	8.0	1.67	3.20	b
R_0	10 ⁻⁸ cm	3.2	3.2	3.2	b
Γ_{PH}	10 ⁹ Hz	25	25	25	b
G	s ⁻¹ K ⁻¹	0.17	0.06	0.10	b
P_N	10 ²⁹ erg ⁻¹ cm ⁻³	4.5	0.36	0.26	c
E_{\max}/k	K	65	130	80	c
γ^d	eV	0.2	0.6	0.1	c
γ^e	eV	0.3	1.4	0.9	c
d	10 ⁻⁸ cm	0.3	0.2	0.1	c

^aCommon parameter values used by Anthony and Anderson (Ref. 19) and in this work.

^bParameter values used in this work only.

^cParameter values from Ref. 19 which differ from those used in this work.

^dResults from thermal-conductivity data.

^eResults from dielectric-susceptibility data.

values estimated by them do describe the results of several different experiments on β -alumina, and we believe that a detailed comparison of the parameters obtained by them and by us reveals similarities which support our model of the F^+ -center relaxation in β -alumina. The temperature dependence observed for any of the experiments is determined by P_M , P_N , and E_{\max}/k . By examining the data of Table I and comparing the relative size of these parameters for each cation, the same trends are observed in both sets of experiments. The magnitudes of these parameters are also in agreement, but due to the normalization of $P(E)$ in our expression of $\langle 1/T_{1F} \rangle$, our model is only sensitive to the relative size of P_M to P_N . We could also have fitted our relaxation data with a constant $P(E)$ by making small changes in the values of E_{\max}/k . The magnitude of our predicted relaxation rate is determined by γ , d , A , and R_0 . These parameters are not independently determined in our model, but it is significant that our theory predicts the observed rate for values of γ and d which are in good agreement with those of Anthony and Anderson.¹⁹ Also, the values of A and R_0 are reasonable when the structure and observed hyperfine couplings in the β -alumina are considered. In comparing the relative values of γd required to fit our data and those of Anthony and Anderson, we note that the same trends can be seen in the relaxation and dielectric-susceptibility data as one changes from cation to cation. This further supports our model of tunneling cations interacting with F^+ centers via contact hyperfine interactions. The estimate of a constant Γ_{PH} results from the weak-field dependence in Fig. 4. The value of $\Gamma_{\text{PH}}/h \approx 25$ GHz is within an order of magnitude of estimated phonon mean free paths in glasses based on thermal-conductivity data. Considering the scatter of the data in Fig. 4, larger values of Γ_{PH} would also be acceptable, producing an even weaker magnetic-field dependence. Another contribution to the

magnetic-field dependence is the dependence of Γ_{PH} upon the phonon energy. This is observed for lower phonon energies^{40,41} and may influence the F^+ relaxation rate at those temperatures where the rate is just becoming temperature dependent. However, the scatter in our data precludes more detailed calculations. The coefficient G of the low-temperature, linear relaxation rate was determined from the lowest-temperature data. Its origin was discussed in Sec. III.

V. CONCLUSIONS AND COMMENTS

The data and model presented here constitute the first quantitative study of electron-spin relaxation in a glass. The LTS-phonon relaxation mechanism we have outlined accurately predicts the magnitude and temperature dependence observed in our electron-spin-relaxation data. The LTS parametrization used to describe our data is in good agreement with previous heat-capacity, thermal-conductivity, and dielectric-susceptibility measurements in β -alumina. In addition, we have inferred that phonon-lifetime effects are responsible for the weak magnetic-field dependence displayed in our data. We have clarified the relationship between the model of Lyo and Orbach,¹⁵ used to describe optical homogeneous linewidth data, and the model we have used to explain our electron-spin-relaxation data.

ACKNOWLEDGMENTS

This work was supported in part by the U. S. DOE under Contract No. EY-76-C-02-1198. The authors also wish to acknowledge helpful discussions and/or assistance from M. M. Abraham, A. C. Anderson, P. J. Anthony, and D. G. Stinson.

- ¹D. W. Feldman, J. G. Castle, Jr., and G. R. Wagner, Phys. Rev. **145**, 237 (1966).
²J. Murphy, Phys. Rev. **145**, 241 (1966).
³J. Szeftel and H. Alloul, Phys. Rev. Lett. **34**, 657 (1975).
⁴J. Szeftel and H. Alloul, J. Non-Cryst. Solids **29**, 253 (1978).
⁵Mark Rubenstein, H. A. Resing, T. L. Reinecke, and K. L. Ngai, Phys. Rev. Lett. **34**, 1444 (1975).
⁶Mark Rubenstein and H. A. Resing, Phys. Rev. B **13**, 959 (1976).
⁷T. L. Reinecke and K. L. Ngai, Phys. Rev. B **12**, 3476 (1975).
⁸G. E. Jellison, Jr., and S. G. Bishop, Phys. Rev. B **19**, 6418 (1979).
⁹P. M. Selzer, D. L. Huber, D. S. Hamilton, W. M. Yen, and M. J. Weber, Phys. Rev. Lett. **36**, 813 (1976).

- ¹⁰J. Hegarty and W. M. Yen, Phys. Rev. Lett. **43**, 1126 (1979).
¹¹P. W. Anderson, B. I. Halperin, and C. M. Varma, Philos. Mag. **25**, 1 (1972).
¹²W. A. Phillips, J. Low Temp. Phys. **7**, 351 (1972).
¹³S. R. Kurtz and H. J. Stapleton, Phys. Rev. Lett. **42**, 1773 (1979).
¹⁴S. R. Kurtz and H. J. Stapleton, in *Fast Ion Transport in Solids*, edited by P. Vashishta, J. N. Mundy, and G. K. Shenoy (North-Holland, Amsterdam, 1979).
¹⁵S. K. Lyo and R. Orbach (private communication).
¹⁶C. R. Peters, M. Bettman, J. W. Moore, and M. D. Glick, Acta Crystallogr. B **27**, 1826 (1971).
¹⁷P. J. Anthony and A. C. Anderson, Phys. Rev. B **14**, 5198 (1976).
¹⁸P. J. Anthony and A. C. Anderson, Phys. Rev. B **16**, 3827 (1977).

- ¹⁹P. J. Anthony and A. C. Anderson, Phys. Rev. B 19, 5310 (1979).
- ²⁰U. Strom, M. von Schickfus, and S. Hunklinger, Phys. Rev. Lett. 41, 910 (1978).
- ²¹Union Carbide Corporation, Crystal Products Division, 8888 Balboa Avenue, San Diego, Calif. 92123.
- ²²P. J. Anthony, Ph.D. thesis (University of Illinois, 1978) (unpublished).
- ²³K. O'Donnell, R. C. Barklie, and B. Henderson, J. Phys. C 11, 3871 (1978).
- ²⁴T. Kaneda, J. B. Bates, and J. C. Wang, Solid State Commun. 28, 469 (1978).
- ²⁵R. C. Herrick and H. J. Stapleton, J. Chem. Phys. 65, 4778 (1976).
- ²⁶D. W. Feldman, R. W. Warren, and J. G. Castle, Jr., Phys. Rev. 135, A470 (1964).
- ²⁷W. M. Rogers and R. L. Powell, Nat. Bur. Stand. (U.S.) Circ. 595 (1958).
- ²⁸J. Jäckle, Z. Phys. 257, 212 (1972).
- ²⁹Michael W. Klein, Baruch Fischer, A. C. Anderson, and P. J. Anthony, Phys. Rev. B 18, 5887 (1978).
- ³⁰A. E. Hughes and B. Henderson, in *Point Defects in Solids*, edited by J. H. Crawford and L. M. Slifkin (Plenum, New York, 1972), Vol. 1; also W. C. Holton and H. Blum, Phys. Rev. 129, 89 (1962).
- ³¹T. J. Schmutge and C. D. Jeffries, Phys. Rev. 138, A1785 (1965).
- ³²A. S. Barker, Jr., J. A. Ditzemberger, and J. P. Remeika, Phys. Rev. B 14, 386 (1976).
- ³³C. H. Hao, L. L. Chase, and G. D. Mahan, Phys. Rev. B 13, 4306 (1976).
- ³⁴D. B. McWhan, C. M. Varma, F. L. S. Hsu, and J. P. Remeika, Phys. Rev. B 15, 553 (1977).
- ³⁵Brage Golding and John E. Graebner, in *Physics of Amorphous Insulators*, edited by W. A. Phillips (Springer-Verlag, Berlin, in press).
- ³⁶S. Hunklinger and W. A. Arnold, in *Physical Acoustics*, edited by W. P. Mason and R. N. Thurston (Academic, New York, 1976), Vol. 12.
- ³⁷J. L. Black and B. I. Halperin, Phys. Rev. B 16, 2879 (1977).
- ³⁸A. Bachelierie, P. Doussineau, A. Levelut, and T.-T. Ta, J. Phys. (Paris) 38, 69 (1977).
- ³⁹Charles Kittel, Phys. Rev. 75, 972 (1949).
- ⁴⁰W. Dietsche and H. Kinder, Phys. Rev. Lett. 43, 1413 (1979).
- ⁴¹M. D. Zaitlin and A. C. Anderson, Phys. Rev. B 13, 4475 (1975).